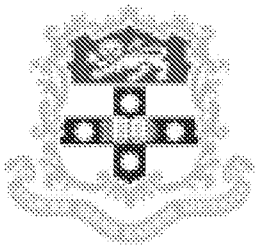

ENERGY METABOLISM IN THE BRAIN AND RAPID DISTRIBUTION OF GLUTAMATE TRANSPORTER GLAST IN ASTROCYTES

KHOA THUY DIEM NGUYEN

A thesis submitted to The University of Sydney in fulfilment of the requirements for the degree of

DOCTOR OF PHILOSOPHY

Department of Anatomy and Histology
The University of Sydney

May, 2008

TABLE OF CONTENTS

DECLARATION

The work presented in this thesis was conducted in Department of Anatomy and Histology (The University of Sydney), Department of Physiology (The University of Sydney), Bosch Institute (The University of Sydney), School of Chemistry (The University of Sydney) and Department of Biomedical Science (The University of Wollongong) by the author otherwise reference is stated.

Khoa T. D. Nguyen

ACKNOWLEDGEMENTS

I would like to thank my supervisor Dr. Vladimir Balcar for his guidance, advice and thoughtful discussion throughout my study. I also wish to extend my gratitude for his teaching of data analysis and his critical appraisal of this manuscript.

I would like to thank my associated supervisor Dr. Ron Clarke for his guidance, technical advice, discussion and partial assessment of the manuscript. Extensive thanks for his support and encouragement me to understand the sequence of experiments.

I would like to thank Prof. Maxwell Bennett for allowing me to use his laboratory to do my experiments.

I wish to thank Assoc. Prof. Paul Else from Department of Biomedical Science, The University of Wollongong, for giving me the opportunity to do my experiments in his laboratory. I would also like to express my gratitude for his discussion and guidance that inspired me to undertake further steps of the experiments.

Many thanks go to Dr. Toby Knight for teaching me the microscope. His patient assistance and encouragement helped me to understand the concept, the instrument and computer technique. I must also thank Dr. Louise Cole for her microscope assistance.

I would like to thank Dr. Vlado Buljan for teaching me the cultures and technical advice in a physical view. I also wish to thank Postgraduate Coordinator Assoc. Prof. Frank Lovicu for his advice and encouragement.

I appreciate the great support and care for me of Assoc. Prof. Mark Vitha from Chemistry Department, Drake University, USA. His encouragement and patience have lifted me up and kept me on track.

Finally, to my son, for understanding and support my study.

ABSTRACT

Glutamate transporters play a role in removing extracellular excitatory neurotransmitter, L-glutamate into the cells. The rate of the uptake depends on the density of the transporters at the membrane. Some studies claimed that glutamate transporters could transit between the cytoplasm and the membrane on a time-scale of minutes. The present study examined the distribution of glutamate transporter GLAST predominantly expressed in rat cortical cultured astrocytes between the membrane and the cytoplasm by using deconvolution microscopy and then analyzing the images. The regulation of the distribution of GLAST was studied in the presence of glutamate transporter substrate (D-aspartate), purinergic receptor activators (α,β-methylene ATP, adenosine), neuroleptic drugs (clozapine, haloperidol), ammonia (hyperammonia) and Na^+/K^+-ATPase inhibitors (ouabain, digoxin and FCCP).

It was demonstrated that the translocation of GLAST towards the plasma membrane was induced by D-aspartate, α,β-methylene ATP, adenosine, clozapine and ammonia (at 100 μM and very high concentrations of 10 mM). However, the inhibition of Na^+/K^+-ATPase activity had an opposite effect, resulting in redistribution of GLAST away from the membrane.

It has previously been claimed that the membrane-cytoplasm trafficking of GLAST was regulated by phosphorylation catalysed by protein kinase C delta (PKC-delta). Involvement of this mechanism has, however, been put to doubt when rottlerin, a PKC-delta inhibitor, used to test the hypothesis showed to inhibit Na^+/K^+-ATPase-mediated uptake of Rb^+, suggesting that rottlerin influenced the activity of Na^+/K^+-ATPase. As Na^+/K^+-ATPase converts ATP to energy and pumps Na^+, K^+ ions, thus helping to maintain normal electrochemical and ionic gradients across the cell membrane. Its inhibition also reduced D-aspartate transport and could impact on the cytoplasm-to-membrane traffic of GLAST molecules. Furthermore, rottlerin decreased the activity of Na^+/K^+-ATPase by acting as a mitochondrial inhibitor. The present study has focused on the inhibition of Na^+/K^+-ATPase activity by rottlerin, ouabain and digoxin in

homogenates prepared from rat kidney and cultured astrocytes. The activity of Na^+/K^+-ATPase was measured by the absorption of inorganic phosphate product generated from the hydrolysis of ATP and the fluorescent transition of the dye RH421 induced by the movement of Na^+/K^+-ATPase. This approach has a potential to test whether the rottlerin effect on Na^+/K^+-ATPase is a direct inhibition of the enzyme activity.

Rottlerin has been found to block the activity of Na^+/K^+-ATPase in a dose-dependent manner in both rat kidney and astrocyte homogenates. Therefore, rottlerin inhibited the activity of Na^+/K^+-ATPase directly in a cell-free preparation, thus strongly indicating that the effect was direct on the enzyme. In parallel experiments, ouabain and digoxin produced similar inhibitions of Na^+/K^+-ATPase activity in rat kidney while digoxin blocked the activity of Na^+/K^+-ATPase to a greater extent than ouabain in rat cortical cultured astrocytes. In a separate set of experiments, Na^+/K^+-ATPase in the astrocytic membrane was found to be unsaturated in $E_1(Na^+)_3$ conformation in the presence of Na^+ ions and this could explain the differences between the effects of digoxin and ouabain on the activity of Na^+/K^+-ATPase in rat astrocytes. In addition, it was found that at low concentrations of rottlerin, the activity of Na^+/K^+-ATPase was increased rather than inhibited. This effect was further investigated by studying rottlerin interactions with membrane lipids.

The activity of Na^+/K^+-ATPase has been reported to be regulated by membrane lipids. The enzyme activity can be enhanced by increasing fluidity of the lipid membrane. I have, therefore, proposed that rottlerin binds to the membrane lipids and the effects of rottlerin on Na^+/K^+-ATPase are mediated by changes in the properties (fluidity) of the membrane. The hypothesis was tested by comparing rottlerin and a detergent, DOC (sodium deoxycholate), for their binding to the lipids by using a DMPC (1,2-Dimyristoyl-sn-Glycero-3-Phosphocholine) monolayer technique. DOC has been shown to both increase and inhibit activity of Na^+/K^+-ATPase in a manner similar to that displayed by rottlerin. The effects of rottlerin and DOC on the DMPC monolayers were studied by measuring the surface pressure of DMPC monolayers and surface area per DMPC molecule. I established that both rottlerin and DOC decreased the surface pressure of

DMPC monolayers and increased the surface area per DMPC molecule. This indicates that both rottlerin and DOC penetrated into the DMPC monolayers. If rottlerin can interact with the lipids, changes in fluidity of the lipid membrane cannot be ruled out and should be considered as a possible factor contributing to the effects of rottlerin on the activity of Na^+/K^+-ATPase.

Overall, the study demonstrates that rottlerin is not only a PKC-delta inhibitor but can have additional effects, both on the enzyme activities (Na^+/K^+-ATPase) and/or on lipid-containing biological structures such as membranes. The findings have implication not only for studies where rottlerin was used as a supposedly specific PKC-delta inhibitor but also for mechanisms of its toxicity.

PUBLICATIONS AND ABSTRACTS

Nguyen K. T. D., Shin J. W., Rae C., Nanitsos E. K., Acosta G. B., Takatsuka M., Pow D. V., Bennett M. R., Clarke R. J., Else P. and Balcar V. J. (2008) Rottlerin inhibits Na^+/K^+-ATPase activity in brain tissue and alters D-aspartate dependent redistribution of glutamate transporter GLAST in cultured astrocytes, in preparation

Shin J. W., **Nguyen K. T. D.**, Takatsuka M., Pow D. V., Knight T., Buljan V., Bennett M. R. and Balcar V. J. (2008) Distribution of glutamate transporter GLAST in membranes of cultured astrocytes in the presence of glutamate transport substrates and ATP, in preparation

Nanitsos E. K., **Nguyen K. T. D.**, St'astný F. and Balcar V. J. (2005) Glutamatergic hypothesis of schizophrenia: Involvement of Na^+/K^+-dependent glutamate transport. *J. Biomed. Sci.* **12**, 975–984

Balcar V. J., **Nguyen K. T. D.**, Shin J. W., Rae C., Nanitsos E. K., Acosta G. B., Pow D. V. and Bennett M. R. Rottlerin inhibits Na^+/K^+-ATPase activity but does not cause redistribution of glutamate transporter GLAST in cultured astrocytes. *Abstracts of 44th Annual Meeting of The American Society for Cell Biology, Washington DC, USA*, pp. 494a, 2004, Abstr. No. 1893

ABBREVIATIONS

$1/\tau_1$	reciprocal relaxation time
2-OG	2-oxoglutarate
5-HT receptors	5-Hydroxytryptamine (serotonin) receptors
ACh	acetylcholine
ADP	adenosine diphosphate
AF 488	Alexa Fluorescent 488
AF 594	Alexa Fluorescent 594
AMP	adenosine monophosphate
AMPA	α-amino-3-hydroxy-5-methyl-4-isoxazolepropionic acid
ANOVA	one way analysis of variance
AOAA	aminooxyacetic acid
ATP	adenosine triphosphate
B_{max}	overall binding capacity
BSA	bovine serum albumin
CaM-kinase III	calmodulin kinase III
cAMP	cyclic adenosine monophosphate
CCS	cosmic calf serum
CNS	central nervous system
CSF	cerebrospinal fluid
DA	dopamine
D-Asp	D-aspartate
dBcAMP	dibutyryl cyclic adenosine monophosphate
DMEM	Dulbecco's Modified Eagle's Medium
DMEMs	DMEM supplemented with 10% CCS and 1% P/S/G
DMPA	dimyristoyl-L-α-phosphatidic acid
DMPC	1,2-Dimyristoyl-sn-Glycero-3-Phosphocholine
DMSO	dimethyl sulfoxide
DOC	sodium deoxycholate
DS	dextran sulfate

EAAC	excitatory amino acid carrier
EAAT	excitatory amino acid transporter
ecto-NTPDases	ecto-nucleoside triphosphate diphosphohydrolases
EDTA	ethylenediaminetetraacetic acid
EPSC	excitatory postsynaptic current
$FADH_2$	reduced flavin adenine dinucleotide
FCCP	carbonyl cyanide p-trifluoromethoxyphenylhydrazone
GABA	γ-aminobutyric acid
GFAP	glial fibrillary acidic protein
GLAST	glutamate-aspartate transporter
GLT	glutamate transporter
HA	hyperammonia
HE	hepatic encephalopathy
HS	horse serum
IC_{50}	concentration of inhibitor causing 50% inhibition
KA receptors	kinate receptors
K_m	Michaelis constant
LTP	long-term potentiation
mACh receptors	muscarinic receptors
mGluRs	metabotropic glutamate receptors
MNV	trigeminal mesencephalic nucleus
NA	numerical aperture
Na_3VO_4	sodium orthovanadate
NADH	reduced nicotinamide adenine dinucleotide
n_H	hill coefficient value
NMDA	N-methyl-D-aspartate
NMR	nuclear magnetic resonance
NTS	solitary tract nucleus neurons
P/S/G	penicillin/streptomycin/glutamine
P1, P2 receptors	purinergic receptors
P2X	ligand-gated cationic channels

P2Y	G-protein-coupled receptors
PBS	phosphate buffered saline
PC	phosphatidylcholine
PE	phosphatidylethanolamine
PFC	prefrontal cortex
pH_i	intracellular pH
P_i	inorganic phosphate
PKC	protein kinase C
PLC	phospho-lipase C
PMA	phorbol 12-myristate 13-acetate
RFI	ratio of fluorescence intensity
RH421	N-(4-sulfobutyl)-4-(4-(p-(dipentylamino)phenyl)butadienyl)pyridinium
sfDMEM	serum-free DMEM
t-3-OHA	threo-3-hydroxyaspartate
TBOA	DL-threo-benzyloxyaspartate
TCA	tricarboxylic acid
T_m	phase-transition temperature
Trizma	triz(hydroxymethyl)aminomethane
T_t	critical temperature
VCH	V. cholerae hemolysin
VGCCs	voltage-gated Ca^{2+} channels
V_{max}	maximal velocity
WD	working distance
α,β-methylene ATP	α,β-methylene adenosine 5'-triphosphate lithium salt
π-A	surface pressure-area
π-Γ	surface pressure-concentration

LIST OF FIGURES

INTRODUCTION

1.1 GLUTAMATE TRANSPORTERS

1.1.1 Glutamate

L-glutamate, an amino acid, is the principal excitatory neurotransmitter in the central nervous system (CNS) of mammals (review: Fonnum, 1984; historical overviews: Bennett and Balcar, 1999; Watkins and Jane, 2006). Glutamate is released from glutamate-containing vesicles in nerve terminals by exocytosis and the interaction with glutamate receptors changes permeability of the neuronal membrane to Na^+, K^+ ions thus resulting in the generation of action potential. Ca^{2+} ions may also be taken up into neurons. Excessive uncontrolled activation of glutamate receptors could damage neurons (review: Rothman and Olney, 1995). Therefore, the extracellular presence of glutamate has to be maintained at a low level. The concentration of glutamate in the cerebrospinal fluid (CSF) probably reflects the extracellular concentration which has been reported around 10 μM (Hamberger and Nyström, 1984). The rapid way to remove glutamate from the extracellular space is by reuptake into neighbouring cells (Balcar and Johnston, 1972). Indeed, a glutamate uptake inhibitor, TBOA (DL-*threo*-benzyloxyaspartate) caused an elevation of the extracellular glutamate within seconds (Jabaudon et al., 1999; for further references see Danbolt, 2001). The uptake of the extracellular glutamate is accomplished by cellular glutamate transporter proteins.

1.1.2 Glutamate transporters

1.1.2.1 Subtypes

Five glutamate transporters have been cloned: EAAT1 (Excitatory Amino Acid Transporter) also called GLAST (Glutamate-Aspartate Transporter), EAAT2 also called GLT (Glutamate Transporter), EAAT3 also known as EAAC (Excitatory Amino Acid Carrier), EAAT4 and EAAT5 (Arriza et al., 1997; Fairman et al., 1995; Storck et al., 1992; Pines et al., 1992; Kanai and Hediger, 1992; reviews: Danbolt, 2001; Balcar, 2002). The most common practice is that the glutamate transporters in animals are

named GLAST, GLT-1, EAACl and EAAT4 whereas their homologues found in human brain are named EAATl, EAAT2, EAAT3 and EAAT4 (Kanai, 1997). The human proteins exhibit amino acid homologies typically of 92-96% to rat and rabbit sequences (Arriza et al., 1994).

1.1.2.2 Structure

The glutamate transporter proteins are structured as oligomeric complexes. It is thought that GLT and EAAC1 are assembled as trimers consisting of three identical subunits. The individual subunit of the trimers functions independently from the neighboring subunits to transport glutamate (Haugeto et al., 1996; Gendreau et al., 2004; Grewer et al., 2005). GLAST exists mainly as dimers (Haugeto et al., 1996). The formation of the trimers which occurred during or after the synthesis of the individual subunits resulted in stable trimers and functional oligomeric state (Gendreau et al., 2004).

1.1.2.3 Function of glutamate transporters and its energetics

The glutamate transporters transport L-glutamate, D-aspartate and L-aspartate and some other amino acids such as threo-beta-hydroxyaspartate, threo-3-hydroxyaspartate (t-3-OHA) and cysteate (Kanai et al., 1996) against steep concentration gradients. The transporters utilize electrochemical gradients as the driving forces to take up the amino acid neurotransmitters into the cells. The transport of one glutamate molecule couples 2 or 3 Na^+ ions, associates with the cotransport of either 1 H^+ ion or the countertransport of 1 OH^- ion and accompanies with the countertransport of 1 K^+ ion. Aspartate was thought to be transported with H^+ (Erecinska et al., 1983) whereas L-glutamate was transported as an anion without H^+ (Gazzola et al., 1981). In the ionic stoichiometry of glutamate transporter GLAST, glutamate is cotransported with 3 Na^+ ions, 1 H^+ ion and counter-transported with 1 K^+ ion (Owe et al., 2006). A study from Kanai et al. (1995) indicated that the transporter EAAC1 transferred 1 glutamate molecule, 2 Na^+ ions, 1 H^+ ion or 1 countertransported OH^- ion. However, other studies showed that 1 glutamate was transported with 3 Na^+ ions, 1 H^+ ion and 1 countertransported K^+ ion for GLT-1 and

EAAT3 glutamate transporters (Levy et al., 1998; Zerangue and Kavanaugh, 1996). In addition to the ions-coupled transport of glutamate transporters, the uptake of glutamate also activates uncoupled chloride conductance through the transporters as glutamate-gated chloride channels (Ryan and Vandenberg, 2005). Five types of glutamate transporters: EAAT1, EAAT2, EAAT3, EAAT4 and EAAT5 showed to flux Cl^- ion in a manner of glutamate dependence (Wadiche et al., 1995; Fairman et al., 1995; Arriza et al., 1997).

1.1.3 Astrocytes and glutamate transporters

1.1.3.1 Astrocytes

Astrocytes, a member of the glial cell family, are involved in regulating the extracellular concentration of neurotransmitter glutamate. Astrocytes have been found to surround the neuronal synaptic cleft (Chaudhry et al., 1995). The presence of astrocytes in the neuronal environment protected neurons from glutamate-induced neurotoxicity (Rosenberg et al., 1992). Glutamate is released from pre-synaptic neurons and taken up mainly by astrocytes. The uptake is mediated by specific transporters. In astrocytes, they are GLT and GLAST whereas EAAC1 and EAAT4 locate on neurons (Rothstein et al., 1994; Chaudhry et al., 1995) and EAAT5 is restricted to the retina (Sims and Robinson, 1999; Danbolt, 2001). Inside an astrocyte compartment, glutamate is converted into glutamine by glutamine synthetase predominantly expressed in astrocytes in the brain (Norenberg and Martinez-Hernandez, 1979). Then, glutamine is released into extracellular fluid and taken up by neurons in which glutamine is converted back to glutamate by neuronal glutaminase (Waniewski and Martin, 1986; Laake et al., 1995; Sibson et al., 1997; Rae et al., 2003). Glutamine, if it leaked into the extracellular space, would be practically harmless whereas extracellular glutamate, particularly at high concentrations, would be neurotoxic (Lucas and Newhouse, 1957).

1.1.3.2 Astroglial glutamate transporters

GLT-1 and GLAST present in astrocytes (astroglial GLT-1 and GLAST transporters) have major roles in removing of the extracellular glutamate and maintaining the extracellular glutamate concentration below neurotoxic levels whereas neuronal EAAC1 and EAAT4 transporters seem to have less effects on the clearance of the extracellular glutamate (Rothstein et al., 1996). The extracellular levels of glutamate could be related directly to the amount of glutamate transporter GLAST and GLT-1 protein in surrounding astrocytic membranes. It has been reported that inhibition of the synthesis of glutamate transporters GLAST and GLT-1 resulted in the reduction of the expression of glutamate transporter protein and the activity of glutamate transporters in vivo and in vitro. Also, a loss of glutamate transporters GLAST and GLT-1 caused an elevation of the extracellular glutamate concentration. The levels of GLAST and GLT-1 protein were reduced, for example after traumatic brain injury (Rao et al., 1998). Elevation of the extracellular glutamate concentration has been observed when the transporter levels were decreased (Rothstein et al., 1996).

Initial studies in cultured cells suggested that in astrocyte cultures, GLAST was the predominantly expressed glutamate transporters (Stanimirovic et al., 1999) whereas GLT-1 had usually little or no role in glutamate uptake (Voutsinos-Porche et al., 2003). In rat cultured astrocytes, the expression of mRNAs for glutamate transporter GLAST was more prominent than for GLT-1 but there were variations depending from which brain region the cells were cultured: cerebrum, hippocampus and brain stem (Kondo et al., 1995). It has been known for some time that glutamate uptake into cultured cells could be increased by culturing in the presence of dibutyryl cyclic adenosine monophosphate (dBcAMP) (Borg et al., 1979). In deed, the expression of GLAST and GLT-1 can be stimulated by a range of factors including dBcAMP or simply by the presence of neurons. Cultured astrocytes exposured to dBcAMP significantly promoted transformation of astrocytes in terms of GLAST, GLT-1 gene expression and GLAST, GLT-1 mRNA levels (Eng et al., 1997). Consequently, dBcAMP induced an elevation in GLAST, GLT-1 protein levels and a higher activity of these transporters (Schlag et al.,

1998). The expression of dBcAMP-induced GLAST was greater than GLT-1 (Eng et al., 1997). The presence of neurons in cultured astrocytes also induced the expression of GLT-1 (Schlag et al., 1998). In other glial cell types, oligodendrocytes and microglia, the expression of mRNA was equal for both GLAST and GLT-1 (Kondo et al., 1995). However, the significance of glutamate transport expression in non-astrocytic types of glial cells is not clear at present.

1.1.4 Activity and cell-surface expression of GLAST

The activity of glutamate transporter GLAST is increased by the presence of the extracellular glutamate and that increase could be a result of a higher density of the transporters as suggested by measuring cell-surface expression of GLAST in primary murine astrocyte cultures (Duan et al., 1999). It indicates that the activity of glutamate transporter GLAST was proportional to the cell-surface expression of GLAST. Many types of membrane-bound proteins can undergo a dynamic trafficking between the intracellular compartments and the cell surface. The change in the cell-surface expression of the transporters in minutes or seconds can regulate the activity of membrane-bound proteins much faster than the regulation of protein synthesis (Duan et al., 1999).

In general, the activation of PKC (protein kinase C) caused a rapid change in the cell-surface expression of neurotransmitter transporters such as GAT1, a subtype of GABA transporters (Beckman et al., 1999), dopamine transporters (Daniel and Amara, 1999; Melikian and Buckley, 1999) and serotonin transporters (Qian et al., 1997). For glutamate transporters, the activation of phorbol ester-induced PKC caused a decrease in the cell-surface expression of GLT-1 in two models: primary co-cultures of neurons and astrocytes that endogenously express GLT-1 and C6 glioma cells transfected with GLT-1 (Kalandadze et al., 2002) whereas the activation of PKC caused an opposite effect on the cell-surface expression of EAAC1 in C6 glioma cells (Davis et al., 1998). The stimulation of glutamate transporters was a direct phosphorylation of the transporters by PKC (Casado et al., 1993). However, the effects of PKC on the redistribution of GLAST

at the membrane are various. The activation of PKC caused a reduction in the cell-surface GLAST immunoreactivity in rat astrocyte cultures (Susarla et al., 2004) and in retinal cultured Müller cells (Wang et al., 2003). In contrast, the activation of PKC had no effect on the cell-surface GLAST expression in Xenopus oocytes or human embryonic kidney cells (Conradt and Stoffel, 1997) and in retinal Müller cells (Bull and Barnett, 2002).

1.1.5 Aims of the study

1/. Observe the unique function of glutamate transporter GLAST as it redistributes between the membrane and the cytoplasm by applying non-metabolized glutamate-analogue D-Asp to rat cortical cultured astrocytes.

2/. Examine the effects of other systems such as purinergic receptors, dopamine receptors, hyperammonia and Na^+/K^+-ATPase on the distribution of GLAST.

1.2 PURINERGIC RECEPTORS

Extracellular ATP has been identified as an excitatory neurotransmitter acting via purinergic receptors (P2 receptors whereas P1 receptors are activated by adenosine). ATP-selective P2 receptors can be divided into two categories: ionotropic, P2X (ligand-gated cationic channels) and metabotropic, P2Y (G-protein-coupled receptors) (Abbracchio and Burnstock, 1994; Ralevic and Burnstock, 1998; North, 2002). The ionotropic P2X receptors and the metabotropic P2Y receptors are widely distributed in the brain (Ralevic and Burnstock, 1998; Abbracchio et al., 2006). The widespread distribution of P2 receptor subtypes was suggested to play the roles in cell differentiation, embryonic development and neurogenesis in physiological conditions (Rathbone et al., 1999; Franke and Illes, 2006; Burnstock, 1996). The P2X receptors are present in neurons located at pre- and post-synapses (Rubio and Soto, 2001; Rodrigues et al., 2005; Rundén-Pran et al., 2005) and in glial cells (Illes and Ribeiro, 2004).

ATP is released into the extracellular space from both neurons and glial cells. In pathophysiological conditions such as hypoxia, ischemia, brain damage, the accumulation of ATP in the extracellular space could be significantly increased. The extracellular ATP is physiologically in the low micromolar concentrations, it can be raised up to millimolar levels after membrane damage, hypoxia or ischemia (Gordon, 1986; Sperlagh and Vizi, 1996; Braun et al., 1998; Melani et al., 2005). The extracellular ATP can be hydrolysed to ADP (adenosine diphosphate) and AMP (adenosine monophosphate) by ecto-NTPDases (ecto-nucleoside triphosphate diphosphohydrolases) and finally to adenosine by ecto-5'-nucleotidases (Zimmermann, 2001). The release of ATP into the extracellular space in physiological conditions contributed to the regulation of neuronal activity (Casel et al., 2005). The activation of purinergic receptors by ATP plays a role in modulating glutamatergic, GABAergic and glycinergic synaptic transmission in the CNS (Deuchars et al., 2001; Gu and MacDermott, 1997; Hugel and Schlichter, 2000; Jang et al., 2001; Khakh and Henderson, 1998; Li et al., 1998; Rhee et al., 2000). Recently, a study has been reported that in cultures of hippocampal neurons, endogenously released ATP suppressed glutamatergic synapses and that effect was dependent on the presence of cocultured astrocytes (Zhang et al., 2003). One year later, Koizumi and Inoue revealed that the release of ATP from astrocytes and the activation of P2 receptors led to a decrease in excitatory glutamatergic synaptic transmission. Some of these findings prompted the present study.

1.2.1 P2X receptors

A subclass of P2 receptors, P2X, contains seven subtypes ($P2X_1$ to $P2X_7$) which have been cloned (North and Surprenant, 2000). The receptor subtypes can be formed as six homomeric subunits ($P2X_1$ to $P2X_5$, $P2X_7$) and at least four heteromeric subunits ($P2X_{2+3}$, $P2X_{4+6}$, $P2X_{1+5}$ and $P2X_{2+6}$) (Khakh et al., 2001; Brown et al., 2002). The subunits have two transmembrane domains, a large extracellular loop containing the ATP binding site and intracellular N and C terminae tails (Khakh et al., 2001). The P2X receptors occur as stable trimers or hexamers of three or six subunits (Nicke et al., 1998; Stoop et al., 1999).

1.2.2 Distribution of P2X receptors

P2X receptor subtypes have been found located at synapses. Synapses expressing P2X receptors were glutamatergic synapses (Yao et al., 2001; Llewellyn-Smith and Burnstock, 1998) and the expression of P2X receptors was dramatically increased in the peripheral part of the synapse compared to the central part of the synapses (Rubio and Soto, 2001). In cultured dorsal root ganglion and spinal dorsal horn neurons, P2X receptors exist on nerve terminals at neuro-neuronal synapses (Gu and MacDermott, 1997). P2X receptors appeared to be localized at presynaptic glutamate terminals on solitary tract nucleus neurons (NTS) (Jin et al., 2004). At postsynaptic membrane, P2X subtypes ($P2X_2$, $P2X_4$ and $P2X_6$) are expressed in CA1 pyramidal cells (Rubio and Soto, 2001). The receptors are also present at both pre- and post-synaptic sites in rat dorsal vagal complex of the brainstem (Ashour and Deuchars, 2004), in the olfactory bulb and cerebellum (Le et al., 1998). In addition, P2X receptors are present on glial cells (Loesch and Burnstock, 1998; Kanjhan et al., 1999; Rubio and Soto, 2001). Primary rat cortical astrocytes express ligand-gated P2X ($P2X_{1\text{-}5}$, $P2X_7$) and G-protein-coupled P2Y receptors ($P2Y_1$, $P2Y_2$, $P2Y_4$, $P2Y_6$, $P2Y_{12}$ and $P2Y_{14}$) (Fumagalli et al., 2003).

1.2.3 Release of extracellular ATP

ATP is released into the extracellular space from both neurons and glial cells. An early finding showed that antidromic stimulation caused ATP to be released from sensory nerves (Holton, 1959). Other studies suggested that ATP may be released in response to neuronal activity (Cunha et al., 1996; Vizi et al., 1997; Sperlagh et al., 1998a). The release of ATP from neurons in brain slices was observed by focal stimulation (Edwards et al., 1992; Hamann and Attwell, 1996) and when nerve endings were depolarized (Sperlágh and Vizi, 1996; Sperlágh et al., 1998b). The released ATP was related with glutamatergic associational fibres (Mori et al., 2001). ATP may also exocytotically secreted in synaptic vesicles with co-storing transmitters such as acetylcholine, noradrenaline, serotonin (Silinsky, 1975; Burnstock, 1986; Richardson and Brown, 1987; von Kügelgen, 1994), GABA (Jo and Schlichter, 1999; Jo and Role, 2002) and glutamate

(Rubio and Soto, 2001). In cultured astrocytes, stimulation of NMDA (*N*-methyl-D-aspartate), AMPA (α-amino-3-hydroxy-5-methyl-4-isoxazolepropionic acid) and (KA) kinate receptors caused ATP to be released into the extracellular space (Queiroz et al., 1999).

1.2.4 Function of P2 receptors

Activation of extracellular ATP-liganded P2 receptors results in a generation of cations inside the cells. Both types of P2X and P2Y receptors can modulate intracellular calcium concentrations by either promoting calcium entry from the extracellular space via P2X receptors (Khakh et al., 2001) or activating phospho-lipase C (PLC), inositol-phosphates formation to release calcium from intracellular stores via P2Y receptors (King et al., 2000). P2X receptors belong to a family of nonselective cation channels gating by extracellular ATP (Jahr and Jessell, 1983; Krishtal et al., 1983; North and Surprenant, 2000). P2X receptors are permeable to Na^+, K^+ and Ca^{2+} ions (Burnashev, 1998).

Functional P2 receptors liganded by extracellular ATP play a role in modulating synaptic transmission. A fast synaptic transmission was mediated by ATP acting at P2X receptors in CA3 pyramidal cells (Mori et al., 2001). ATP increased spontaneous excitatory postsynaptic current (EPSC) frequency (Jin et al., 2004). ATP-evoked increase in EPSC frequency with no change in amplitude suggested that ATP affected the presynaptic processes of transmitter release (Lena and Changeux, 1997). On the other hand, the presence of extracellular ATP in the synaptic clefts contributed to synaptic transmission by activating postsynaptic P2X receptors (Pankratov et al., 2002; Zhang et al., 2003; Khakh, 2001).

1.2.5 The present study

Even though activating P2 receptors by ATP had the effects on fast synaptic transmission, recently, a number of studies have revealed that the activation of P2 receptors from endogenously released ATP suppressed glutamatergic synapses, and the

effects were dependent on the presence of astrocytes (Zhang et al., 2003; Koizumi and Inoue, 2004). In the present study, we intend to measure the contribution of astrocytes in modulating synaptic transmission via P2X receptors by quantifying the distribution of glutamate transporter GLAST in rat cultured astrocytes in the stimulation of P2X receptor subtypes.

1.3 DOPAMINE RECEPTORS

Dopamine (DA) is a monoamine transmitter and a neuromodulator in the CNS. Disruption of dopaminergic functions can result in a number of diseases. Dopamine acts on DA receptors (including D1- and D2-like receptors). There is evidence that dopaminergic functions are disrupted in schizophrenia. However, current thinking favours glutamatergic malfunction as the main cause of schizophrenia. Glutamate transport, in particular, could be changed (review: Nanitsos et al., 2005). Most of the antipsychotic drugs are active as dopamine receptor (D2) antagonists. Is it possible that some of these drugs actually alter the activity of glutamate transporters? Two classes of antipsychotic drugs, including clozapine and haloperidol, used to treat schizophrenia have been reported to produce different effects and side effects on the treatment. This study aims to compare the effects of these two drugs on the distribution of the glutamate transporter GLAST between cellular membrane and cytoplasm in rat cortical cultured astrocytes.

1.3.1 Dopamine

Dopamine is necessary for normal physiological function of the brain. Dopamine has been shown to be released in the prefrontal cortex (PFC) by the stimulation of the hippocampus (Gurden et al., 2000). In rats, normal working memory requires optimal levels of dopamine in the prelimbic area (i.e. rat PFC) (Zahrt et al., 1997; Mizoguchi et al., 2000). In monkeys, interruption of dopaminergic transmission in dorsolateral PFC by focal D1 antagonist application impaired spatial working memory (Sawaguchi and Goldman-Rakic, 1991; 1994). In rodents, dopamine depletion exhibited motor

impairments (Bures and Bracha, 1990) which could be attributed to motor cortex dysfunction, such as deficient temporal sequencing of complex, skilled motor tasks (Salamone et al., 1990; Whishaw et al., 1986) and diminished accuracy and rate of skilled movements (Sabol et al., 1985; Whishaw et al., 1986). Dopamine has been implicated in several psychiatric disorders including schizophrenia, attention deficit hyperactivity disorder, and Tourette's Syndrome (Barkley, 1998; Lewis and Lieberman, 2000; Swanson et al., 1998; Todd and O'Malley, 2001; Weickert et al., 2000; Weinberger, 1999). Several brain areas involved in these diseases including cortical, limbic structures and hippocampus.

1.3.2 Dopamine receptors

Five subtypes of dopamine receptors have been identified and categorized as D1-like (including D1a and D5 receptors) and D2-like (including D2, D3 and D4 receptors) (Civelli et al., 1993; Gingrich and Caron, 1993). They are G-protein-coupled receptors, monomers with seven transmembrane domains (Grandy et al., 1991; Jackson and Westlind-Danielson, 1994). Activation of a G-protein hydrolyses guanosine triphosphate. The G-protein dissociates and activates an effector protein which is an enzyme or an ion channel that either produces an intracellular second messenger (e.g. cyclic adenosine monophosphate (cAMP), inositol triphosphate or arachidonic acid) or causes ion fluxes (Gerfen et al., 1990; Gingrich and Caron, 1993). The activation of D1-R results in a stimulation of adenylyl cyclase whereas the activation of D2-R results in an inhibition of adenylyl cyclase, suggesting that the two types elicit different postsynaptic responses (Albert et al., 1990; Kebabian and Calne, 1979; Neve et al., 1989; Seeman and Van Tol, 1994). Adenylyl cyclase is an enzyme responsible for the production of the second messenger cAMP (Jackson and Westlind-Danielson, 1994).

1.3.3 Modulation of synaptic transmission

Dopamine plays a role in regulating synaptic transmission by either inhibition or stimulation of neuronal activities. In an electrophysiological study, activation of D1 receptors resulted in a reduction of excitatory transmission in collateral synapses between a pair of layer V pyramidal neurons (Gao et al., 2001). In rat PFC slices, dopamine inhibited glutamatergic transmission at layer V pyramidal neurons after stimulation of the superficial (Law-Tho et al., 1994; 1995; Otani et al., 1998; 1999) or deep layer fibers (Law-Tho et al., 1994). In vivo studies, the synaptic transmission in the hippocampo-PFC monosynaptic connection was inhibited by dopamine (Jay et al., 1995; Gurden et al., 1999; Floresco and Grace, 2003). However, in the anesthetized intact brain, dopamine released from dopaminergic axon terminals in the prefrontal cortex facilitated long-term potentiation (LTP) (Otani et al., 2003). Both inhibitory and excitatory responses are induced by dopamine in neurons of the prefrontal and motor cortices, although inhibitory responses predominate (Bernardi et al., 1982; Bradshaw et al., 1985; Sawaguchi et al., 1986a).

1.3.4 Schizophrenia

Schizophrenia is a severe and chronic mental illness (or a group of illnesses) associated with high prevalence (0.5% to 1% of the population suffers from this condition) (*DSM-IV,* 1994). Although the fundamental pathology of schizophrenia remains unclear, a number of studies suggest that changes in several neurotransmitter systems are involved in the pathophysiologic processes of the disease. Disturbances in dopamine and glutamate systems have attracted greatest attention as the causes of the disease. In 1963, Carlsson and Lindqvist proposed a hypothesis of hyperactivity of dopamine transmission in schizophrenia. Later, dopamine hyperfunction has been implicated in schizophrenia (Gray et al., 1995; Joyce, 1993; Joyce and Meador-Woodruff, 1997). Most of the evidences supporting the dopaminergic hypothesis were based on the observations that the early neuroleptics were all blockers of dopamine receptors (Carlsson and Lindqvist, 1963).

However, several studies have demonstrated involvement of the excitatory amino acid neuronal systems in the pathophysiology of schizophrenia (Carlsson and Carlsson, 1990a; Grace, 1991; Olney, 1990; Wachtel and Turski, 1990). Schizophrenia is a glutamatergic deficiency disorder (Carlsson and Carlsson, 1990b; Sherman et al., 1991). The dysfunction of glutamate transmission in schizophrenia involving NMDA receptors has been supported by a number of studies (Olney and Farber, 1995; Javitt and Zukin, 1991; Tamminga et al., 1995; Goff and Coyle, 2001; Jentsch and Roth, 1999). A disruption of one of the systems may affect the function of the other. Clinical and imaging studies suggested that dysregulation of dopamine systems in schizophrenia may be secondary to a deficit in function of NMDA receptors (Olney and Farber, 1995; Miller and Abercrombie, 1996; Kegeles et al., 2000). The disturbance of glutamatergic neuronal systems regulating dopaminergic cell activity caused an increase in amphetamine-induced dopamine release in schizophrenia (Kegeles et al., 2000).

1.3.5 Antipsychotic drugs

Two major categories of antipsychotic drugs used for treatment of psychosis are classical neuroleptic drugs including haloperidol and atypical neuroleptic drugs including clozapine which behave differently on the outcome of the treatment. The treatment of psychosis with neuroleptic drugs is the most common therapeutic strategy (Meltzer, 1999; Kane, 1999). An important common feature of neuroleptic drugs is an ability to block brain dopamine receptors (Carlsson and Lindqvist, 1963). Atypical neuroleptic drugs exert fewer side effects than classical antipsychotic agents (Farde et al., 1992; Meltzer and McGurk, 1999). Atypical antipsychotic agents show less motor function impairment whereas classical neuroleptic drugs cause severe extrapyramidal side effects, as drug-induced Parkinsonism and tardive dyskinesia (Kane, 1999). The physiological difference between actions of classical and atypical antipsychotic agents has not yet been clarified.

1.3.6 The present study

The treatment of psychosis by haloperidol and clozapine seems to produce different effects on the extracellular glutamate concentrations. In the prefrontal cortex, acute administration of antipsychotic drugs selectively increases extracellular concentrations of glutamate (Pehek et al., 1991; Daly and Moghaddam, 1993). In striatum, acute haloperidol administration results in higher tissue content levels of glutamate whereas acute clozapine administration decreased glutamate concentrations (Bardgett et al., 1993). The extracellular glutamate concentrations are regulated by the major uptake of glutamate transporters expressed in astrocytes which locate at nearby neuronal synapses. The aims of this study are to examine the effects of haloperidol and clozapine on the distribution of glutamate transporter GLAST between cellular membrane and cytoplasm in rat cortical cultured astrocytes.

1.4 AMMONIA

Disturbances of ammonia metabolism resulting from such metabolic disorders as urea cycle enzymopathies, Reye Syndrome, and liver failure are associated with severe neurological impairment. Increased brain concentrations of ammonia are consistent with findings in many neurological disorders including mental retardation, seizures, metabolic coma and increased brain glutamate in the extracellular space where brain ammonia may attain millimolar concentrations (Swain et al., 1992b). Ammonia is principally metabolized and detoxified by astrocytes in the brain (Norenberg, 1995) and its metabolism is closely interrelated with glutamate. Ammonia reacts with glutamate to produce glutamine in astrocytes (Sonnewald et al., 1997). As liver function deteriorates, a severe neuropsychiatric disorder known as hepatic encephalopathy (HE) develops. There are growing evidences that HE and hyperammonemia (causing pathologically high levels of ammonia in brain tissue, too) are associated with de-arrangements in glutamate neurotransmission (Albrecht, 1998; Michalak et al., 1997; Norenberg et al., 1997). The pathology of HE and hyperammonia is dominant in astroglial changes, and inconsistent in neuronal abnormalities (Norenberg, 1995; Jayakumar et al., 2006). The present study

focuses on the distribution of cell-surface glutamate transporter GLAST expressed in rat cultured astrocytes in a condition of acute hyperammonia. The actual cause of hyperammonia symptoms and the fatal outcome of HE are not very well understood.

1.4.1 Presence of ammonia in the brain

Ammonia is accumulated in the brain by an entry via a blood-brain barrier and a release from active neurons. Large quantities of ammonia normally enter the portal vein circulation from protein digestion in the gastrointestinal system. However, arterial ammonia levels are maintained at low concentrations (50 – 100 μM), which illustrate the normal efficiency of the liver to remove gut-derived ammonia. Reduced hepatic capacity for ammonia removal associated with inherited urea cycle disorders or liver injury results in hyperammonemia and spectrum of neuropsychiatric symptoms (Felipo and Butterworth, 2002). Ammonia enters the brain from blood by diffusion rather than via a saturable transport system (Cooper et al., 1979). The blood-brain barrier transfer of ammonia is dependent upon arterial blood pH (Warren, 1958). Also, ammonia is released from neurons where ammonia is generated from the conversion of glutamine to glutamate by catalyzed enzyme glutaminase.

$$\text{Glutamine} + H_2O \rightarrow \text{glutamate} + NH_4^+$$

In vivo, brain ammonium content can be doubled in a few seconds with electrical stimulation or even after a conditioned reflex (Tsukada, 1966). A reduction in neuronal activity is associated with decreased ammonia levels while elevated ammonia levels are observed with intense neuronal activity (Benjamin, 1982).

1.4.2 Mechanisms of ammonia transport into astrocytes

$$NH_4^+ \leftrightarrow NH_3 + H^+$$

Ammonia exists either as the non-ionized ammonia gas (NH_3) or as the ionized, protonated ammonium ion (NH_4^+). The non-ionized form is a readily diffusible molecule (Roos and Boron, 1981). The ionized form does not readily pass cell membranes and can do so only by transporters (Flessner et al., 1992; Lande et al., 1994). The pKa of ammonia is 9.0 and 98.3% of ammonia exists at physiologic pH (7.4) as the ionized NH_4^+ ion. The distribution of total ammonia across cell membranes is determined solely by its pKa, extracellular pH and intracellular pH (Boron and De Weer, 1976; Cooper and Plum, 1987; Roos and Boron, 1981; Szerb and Butterworth, 1992). NH_3 has a high solubility in water and is weakly soluble in lipids. The partition coefficient is < 0.05 (Marcaggi, 1999). The diffusion of NH_3 is primarily responsible for the rapid distribution of ammonia across the astrocyte plasma membrane (Cooper and Plum, 1987). NH_3 enters the cells much more readily than NH_4^+ does in a study of the osmolysis of erythrocytes (Jacobs, 1924). Cytosolic buffering prevents any effects on the intracellular pH at physiologic ammonia concentrations (0.1 – 0.2 mM) (Nagaraja and Brookes, 1998).

However, hyperammonia can cause intracellular acidification in astrocytes. In primary cultures of mouse cerebral astrocytes, the application of 20 mM NH_4Cl caused a typical alkalinization, but this reversed abruptly within a few seconds to be replaced by an intense sustained acidification (Nagaraja and Brookes, 1998). Transmembrane fluxes of NH_3 far exceed fluxes of NH_4^+ in most cells, as evidenced by the rapid intracellular alkalinization detected when the cells are exposed to a high concentration of NH_4Cl (Roos and Boron, 1981). The later acidic phase results from the entry of NH_4^+ into the cells. Because the hydrated ionic radius of NH_4^+ is similar to that of K^+, significant influx of NH_4^+ is observed via nominally K^+-selective channels and transporters (Hille, 1992). A possible mechanism of this somewhat paradoxical effect is that the diffusion coefficients of K^+ and NH_4^+ are almost equal and NH_4^+ can compete with K^+ on membrane ion channels and transporters.

The sensitivity of NH_4^+-induced acidification was inhibited by low concentrations of Ba^{2+} (Ransom and Sontheimer, 1995) strongly suggested that passive influx via K_{ir} channels is the primary entry route for NH_4^+. Also, one-third of the initial rate of acidification elicited by 1 mM NH_4^+ was inhibited by bumetanide, suggesting that the Na^+-K^+-$2Cl^-$ cotransporter also plays a significant role in mediating NH_4^+ entry (Good, 1994; Keicher and Meech, 1994). Nagaraja and Brookes (1998) reported that the combined action of Ba^{2+} and bumetanide eliminated the net acidification by 1 mM NH_4^+ in mouse cortical cultured astrocytes. The authors interpreted that as an intense influx of NH_4^+ persists after the steady-state distribution of ammonia was attained. Once a steady-state distribution of ammonia is reached, all the NH_3 formed by dissociation of entering NH_4^+ during the steady-state will diffuse out, and this cycle of NH_4^+ influx and NH_3 efflux imposes a continuing intracellular load.

1.4.3 Glutamine formation

The formation of glutamine from glutamate and ammonia is catalyzed by glutamine synthetase located in astrocytes. Glutamine synthetase is located specifically in astrocytes (Norenberg and Martinez-Harnandez, 1979). Astrocytes are responsible for a major part of glutamate uptake and metabolism in the brain (Schousboe, 1981). Glutamate can be metabolized via the tricarboxylic acid (TCA) cycle in astrocytes (Farinelli and Nicklas, 1992; Waniewski and Martin, 1986; Yu et al., 1982; Yudkoff et al., 1986; Zielke et al., 1989). When glutamate is taken up into the cells, it can be converted into glutamine, a process consuming ATP. Alternatively, glutamate can function as a substrate for the TCA cycle (Dennis et al., 1976) after conversion to 2-oxoglutarate (2-OG) which can therefore be used for energy production. Glutamate metabolism through the TCA cycle is an energy and ammonia producing pathway. Glutamate concentrations below 0.1 mM, 83% of the glutamate were directly converted to glutamine whereas glutamate concentrations at 0.5 mM, the direct conversion to glutamine was only 43% even though glutamine formation was increased more than two-fold in the presence of 0.5 mM glutamate concentrations (Sonnewald et al., 1997). The authors described that at glutamate concentrations below 0.2 mM, the ammonia cycling

between astrocytes and neurons is sufficient to allow for adequate glutamine synthesis. However, at high glutamate concentrations, deamination of glutamate to 2-OG will thus be a pathway to produce ammonia for glutamine synthesis.

A prerequisite for entry of exogenous glutamate into the TCA cycle is the conversion of glutamate to 2-OG, which can take place via a transamination or a deamination. An increase in the ammonia concentration was observed when transamination reactions were blocked by aminooxyacetic acid (AOAA), indicating that part of the glutamate did enter through transamination but deamination for ammonia production by glutamate dehydrogenase was capable to compensate (Sonnewald et al., 1997). The carbon skeleton of extracellular glutamate is largely converted to lactate and aspartate (Sonnewald et al., 1993). Glutamate enters the TCA cycle via 2-OG for conversion to metabolites like malate and oxaloacetate. Malate can be converted to pyruvate by both cytosolic and mitochondrial malic enzyme, whereas oxaloacetate can be converted to pyruvate by the converted action of phosphoenolpyruvate carboxykinase and pyruvate kinase (Sonnewald et al., 1997). Subsequently, pyruvate may be metabolized to lactate, alanine and acetyl-CoA. Lactate formation from glutamate increased with increasing glutamate concentrations (McKenna et al., 1996). Oxaloacetate can be transaminated to aspartate by aspartate aminotransferase.

Different concentrations of glutamate have different effects on energy phosphate levels of the cells. Incubation with 0.05 mM or 0.25 mM glutamate, ATP content was unchanged in astrocyte cultures (Yu et al., 1982; Yudkoff et al., 1986). In the presence of 0.5 mM glutamate concentrations, high energy phosphate levels were found to be decreased. However, either in the presence of the transaminase inhibitor AOAA or the glutamine synthetase inhibitor methionine sulfoximine, the reduced energy phosphate levels were unchanged further, conceiving that the Na^+/K^+-ATPase consumes more ATP than can readily be resynthesized (Sonnewald et al., 1997).

1.4.4 Hepatic encephalopathy and glutamate systems

Hepatic encephalopathy associated with liver failure and other hyperammonemia pathologies has been addressed and found to be consistent with increased extracellular levels of glutamate. HE in acute liver failure displays a rapid progression and is characterized by brain edema, increased intracranial pressure and, if not treated promptly by liver transplantation, a high mortality rate. HE in chronic liver failure (cirrhosis), generally referred to as portal-systemic encephalopathy, has a slower course starting with alterations of personality and sleep patterns progressing through motor incoordination, stupor and coma (Chan and Butterworth, 1999). Acute HE is produced by thioacetamide hepatotoxicity (Norenberg et al., 1997) and ischemic liver failure (Knecht et al., 1997). At coma stages of encephalopathy in animals with acute liver failure, brain ammonia concentrations were as high as 1 -5 mM (Swain et al., 1992a, b). In both acute and chronic liver failure, brain ammonia concentrations were increased and may attain millimolar levels (Butterworth et al., 1988).

Hyperammonia associated with liver failure resulted in elevated levels of extracellular glutamate in the brain (Michalak et al., 1996; Lavoie et al., 1987). In animal models of HE, the extracellular glutamate concentrations were two to three times higher than normal (De Knegt et al., 1994; Michalak et al., 1996; Moroni et al., 1983). The increased extracellular glutamate levels could reflect increased presynaptic release of glutamate or decreased uptake of released transmitter by Na^+-dependent glutamate transporters. In vivo, the release of glutamate from the cerebral cortex of portacaval-shunted rats was demonstrated to be significantly increased (Moroni et al., 1983). Bosman et al. (1991) showed that glutamate release was increased in brains of rats with experimental hepatic encephalopathy. As well as, a reduction of glutamate uptake when ammonia levels are raised has been seen in cultured astrocytes after prolonged exposure to ammonia (Bender and Norenberg, 1996), in bulk-isolate astrocytes derived from rats with acute liver failure (Albrecht et al., 1988), in synaptosomes from animals with experimental liver failure (Oppong et al., 1995), and in brain slices from patients dying in HE (Schmidt et al., 1990).

Ammonia has been reported to have effects on glutamate receptors. A selective loss of NMDA sites has been found in brains of rats with experimental porto-caval shunt (Peterson et al., 1990). A significant reduction of non-NMDA receptor site densities was also found to be reduced in brains of dogs with congenital portal-systemic encephalopathy (Maddison et al., 1991).

Even though hyperammonemia causes the elevation of the extracellular glutamate, the total brain glutamate levels are decreased. In both acute and chronic hyperammonemias, total brain glutamate concentrations are decreased (Lavoie et al., 1987; Ratnakumari et al., 1994). In animals and in post-mortem brains of patients dying in HE resulting from either acute or chronic liver failure, the total brain glutamate level is reduced (Bosman et al., 1992; Lavoie et al., 1987; Record et al., 1976).

1.4.5 The present study

Contrast to the chronic effects of hyperammonia on glutamate uptake by glutamate transporters, the acute hyperammonia induces higher glutamate uptake into the cells. Acute ammonia treatment (up to 10 min) resulted in increased glutamate uptake in cultured astrocytes (Bender and Norenberg, 1996). Acute exposure to hyperammonia on glial cells isolated from the Salamander retina resulted in higher glutamate uptake by glutamate transporter GLAST (Mort et al., 2001). Bulk-isolated cerebellar astrocytes derived from rats with acute ammonia toxicity showed increased glutamate uptake (Rao and Murthy, 1991). The increase was due to an increase in V_{max} with K_m remaining unchanged. These observations emphasize the greater uptake of glutamate by astrocytes in a condition of acute exposure to hyperammonia. Rao and Murthy (1991) have demonstrated that the increase in glutamate uptake was associated with the greater densities of glutamate transporters. The present study examines the distribution of GLAST between the membrane and the cytoplasm in rat cortical cultured astrocytes exposed to acute hyperammonia.

1.5 Na^+/K^+-ATPase

Na^+/K^+-ATPase is an ATP-consuming enzyme which regulates the transmembrane Na^+ and K^+ distribution. Na^+/K^+-ATPase consists of α and β subunits, which present distinct isoforms in different tissues and cells (Sweadner, 1979; Mercer, 1993). In addition, the enzyme has a third nonobligatory subunit, γ, expressed predominantly in the kidney (Mercer et al., 1993). Recently, the crystal structure of the pig renal Na^+/K^+-ATPase has been identified (Morth et al., 2007). The function of Na^+/K^+-ATPase is useful for the maintenance of osmotic stability of the cells where Na^+ is largely in the extracellular fluid and K^+ is largely in intracellular medium. In one cycle of the enzyme activity, Na^+/K^+-ATPase pumps out three Na^+ ions and pumps in two K^+ ions. The activity of Na^+/K^+-ATPase can be regulated by a number of factors such as Na^+/K^+-ATPase inhibitors, ATP contents or membrane lipids. A decrease in Na^+/K^+-ATPase activity has been observed in some diseases (Rapport et al., 1975; Haglund et al., 1985; Ellis et al., 2003). Consequently, elevated extracellular glutamate concentrations are built up. The present study focuses on the effects of Na^+/K^+-ATPase inhibition on the distribution of glutamate transporter GLAST at the membrane of rat cortical cultured astrocytes.

1.5.1 Structure and function of Na^+/K^+-ATPase

There are four known α-subunit isoforms (α1, α2, α3 and α4) and three known β-subunit isoforms (β1, β2 and β3) (Blanco and Mercer, 1998) and two known γ-subunit variants (γ_a and γ_b) (Küster et al., 2000; Sweadner and Rael, 2000). The larger α subunit is the catalytic subunit and carries a site for ATP binding and phosphorylation (Sweadner, 1989). The α1 isoform is identified in all cells and has been considered as the "housekeeping" enzyme (McDonough et al., 1992). The α1 mRNA is the predominant isoform in rat kidney (Orlowski and Lingrel, 1988). The α2 and α3 isoforms have a more limited distribution. The α3 isoform is located predominantly in neural tissue while the α2 isoform is present in neural tissue and heart ventricles and is also the predominant isoform in adult skeletal muscle (Sweadner, 1979; Mercer, 1993; McDonough et al., 1992; Noël and Godfraind, 1984). In addition, an isoform (α4) has been recently found

in the testis (Shamraj and Lingrel, 1994). In the brains, the expression of α1 mRNA is found predominantly in cerebral cortex, α3 mRNA is found predominantly in pyramidal neurons in the deep layers of cerebral cortex (Hieber et al., 1991). Filuk et al. (1989) found α3 mRNA in deep cortical layers and subcortical structures and α1 mRNA mainly in superficial layers of cortex. The smaller β subunit is glycosylated and is hypothesized to be important for insertion and assembly of the protein in the membrane (Shull et al., 1985; Geering, 1990).

Na^+/K^+-ATPase composes of α and β subunits in a 1:1 stoichiometry (Jørgensen, 1982). Most neurons exhibit expression of α3- and β1-subunits whereas glial cells express α2- and β2-subunits. These results suggest the potential for α1/β1, α3/β1 (neurons) and α1/β2, α2/β2 (glia) subunit combinations (Watts et al., 1991). At least, three α-subunit isoforms (α1, α2 and α3) and two β-subunit isoforms (β1 and β2) have been identified in rat brain (Sweadner, 1989; Mercer, 1993; Lingrel and Kuntzweiler, 1994). In rat cortical cultured astrocytes, there is the presence of α1, α2, β1 and β2 isoforms at the mRNA and protein levels (Hosoi et al., 1997). The ratio of the α1 and α2 isoforms in the cells might be estimated to be about 4:1 (Matsuda et al., 1993).

The γ-subunit functions as ion transport regulators or channels (Sweadner and Rael, 2000). Expression of γ-subunit in a human embryonic kidney cell line has been shown to increase Na^+/K^+-ATPase affinity for ATP in vitro (Pu et al., 2001; Therien et al., 1997; Therien et al., 1999). However, the coexpression of γ-subunit with α- and β-subunits in a rat kidney cell line reduced the Na^+/K^+-ATPase apparent affinity for Na^+ and K^+ in vitro (Arystarkhova et al., 1999). In the absence of α subunit, γ has been shown to form an ion channel (Minor et al., 1998).

Na^+/K^+-ATPase plays a role in generating an electrochemical potential gradient for Na^+ which maintains cellular excitability and drives the Na^+-coupled transport of many ions and small molecules, including Ca^{2+}, glucose and amino acid (Ullrich, 1979).

1.5.2 One cycle of Na^+/K^+-ATPase activity

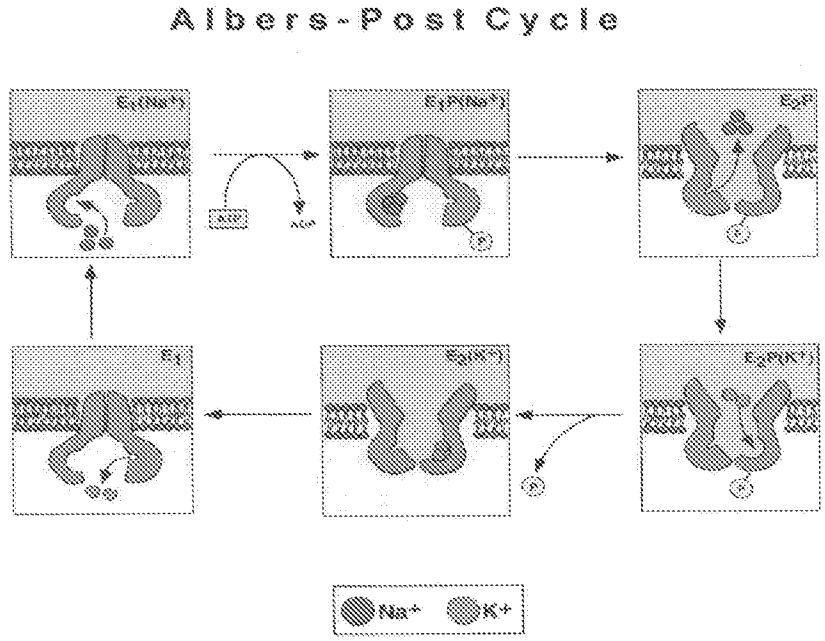

Figure 1.1: A model of one Na^+/K^+-ATPase cycle (called Albers-Post scheme)

Activity of Na^+/K^+-ATPase requires three Na^+ ions, one ATP molecule, one Mg^{2+} ion and two K^+ ions. Three Na^+ ions bind to high affinity binding sites of the Na^+/K^+-ATPase at intracellular surface of $E_1(Na^+)$ conformation. The phosphorylation of the enzyme via the enzyme-binding ATP and Mg^{2+} complex results in $E_1P(Na^+)$ conformation. The Na^+/K^+-ATPase is phosphorylated by ATP which binds to a high affinity site of the enzyme (Albers et al., 1963). The presence of Na^+ ions and ATP molecules increase the phosphatase activity of the enzyme and increase the high affinity for K^+ ions (Nagai and Yoshida, 1966). In the absence of Na^+ ions and ATP molecules, K^+ ions act with low affinity (Drapeau and Blostein, 1980).

Also, the phosphorylation of the enzyme requires both Mg^{2+} and Na^+ ions which must be present at intracellular surface of the enzyme (Blostein et al., 1979). Fukushima and Post (1978) found that the Mg^{2+} ion bound to the enzyme when it was phosphorylated. The release of the ADP molecule causes a change in conformation of the enzyme from $E_1P(Na^+)$ to E_2P and Na^+ ions are released into extracellular medium. The addition of

ADP leads to the disappearance of the phosphorylation of the enzyme and blocks the conversion of $E_1P(Na^+)$ into E_2P. Also, the reduction of Mg^{2+} ion concentrations slows the conversion of the enzyme from $E_1P(Na^+)$ to E_2P. Two K^+ ions bind to high affinity sites on Na^+/K^+-ATPase at the extracellular surface of the $E_2P(K^+)$ conformation of the enzyme and cause dephosphorylation of the enzyme and its conversion into the $E_2(K^+)$ conformation. Absence of Na^+ ions decreases the concentration of $E_2(K^+)$ conformation (Nagai et al., 1966). Then, the binding of ATP to a low affinity at cytoplasmic site stimulates the conformational change and K^+ ions are released into the intracellular medium. ATP accelerates the rate of the conversion of $E_2(K^+)$ to the $E_1(Na^+)$ conformation, acting with a low affinity and without phosphorylation (Karlish and Yates, 1978).

1.5.3 Regulation of Na^+/K^+-ATPase activity

Activity of Na^+/K^+-ATPase relies on the substrate ATP. It is inhibited by cardiac glycosides such as ouabain and digoxin but also by other compounds such as rottlerin. As well as, the activity of Na^+/K^+-ATPase has been reported to be modified by environmental membrane lipids.

1.5.3.1 ATP

The activity of ATPase declines when the ATP concentration is less than 0.4 mM estimated by Dagani and Erecinska (1987). ATP can be generated by processes called glycolysis or mitochondrial oxidative phosphorylation (Garrett and Grisham, 1999). The degradation of glucose (glycolysis) occurs in the cytoplasm of cells. Glycolysis comprises two phases. In phase 1, glucose is broken into two glyceraldhyde-3-phosphate molecules which is then converted into two molecules of pyruvate (phase 2). The additional products of glycolysis are two molecules of ATP and $NADH/FADH_2$ (reduced nicotinamide adenine dinucleotide/ reduced flavin adenine dinucleotide). The further metabolism of pyruvate depends on the aerobic or anaerobic pathways. In the anaerobic pathway, in mammalian cells, pyruvate is reduced into lactate by lactate dehydrogenase

in cytoplasm. In the presence of oxygen, pyruvate is converted into Acetyl-CoA that enables to enter the mitochondrial tricarboxylic acid cycle. The products of this cycle are ATP and NADH/$FADH_2$. Electrons generated by the oxidation of TCA-produced NADH/$FADH_2$ pass through the electron transport pathway to O_2, a final electron acceptor. During the electrons are transferred by the electron transport pathway, protons cross the inner mitochondrial membrane into intermembrane space and establish the proton gradient which drives ATP synthase to synthesize ATP production. The process for the generation of ATP is called mitochondrial oxidative phosphorylation. ATP is an energy substrate for cellular protein enzymes.

1.5.3.2 Ouabain and digoxin

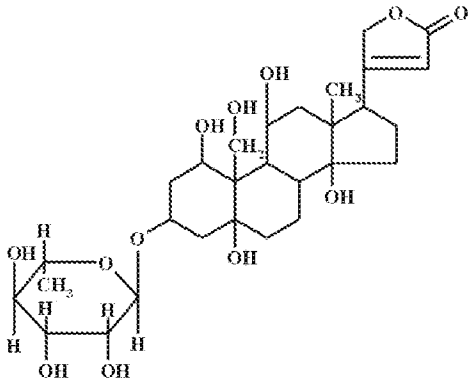

Figure 1.2: Structure of ouabain

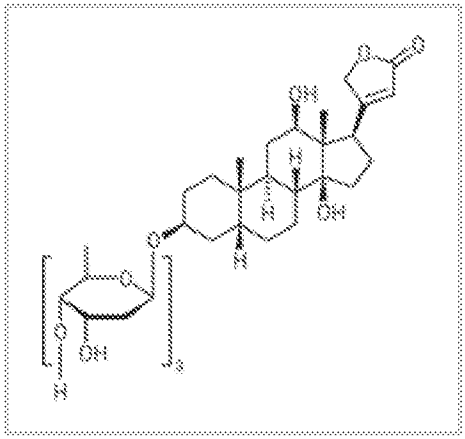

Figure 1.3: Structure of digoxin

Ouabain and digoxin, substances of plant origin, inhibit Na^+/K^+-ATPase activity by binding to an extracellular portion of the Na^+/K^+-ATPase α-subunit (Lingrel et al., 1994). Cardiac glycoside ouabain was identified in human plasma and the adrenal gland (Hamlyn et al., 1991; Sich et al., 1996). Digoxin was shown to be present in human urine (Goto et al., 1990). The characteristic of cardiac glycosides is their toxicity to various animals greatly different between species. Rat α1 isoform of the Na^+/K^+-ATPase is 1000 times more resistant to ouabain than α1 isoforms in other species such as sheep, human and dog (Wallick et al., 1980; Periyasamy et al., 1983). The species-related differences in sensitivity to cardiac glycosides are due to differences in the interaction of these drugs with the Na^+/K^+-ATPase (Gupta et al., 1986). Also, cardiac glycoside ouabain has different sensitivity to different α-subunit isoforms of Na^+/K^+-ATPase. The order of ouabain affinity between the rat α isoforms of the Na^+/K^+-ATPase is α3 > α2 > α1 (O'Brien et al., 1994).

1.5.3.3 Rottlerin

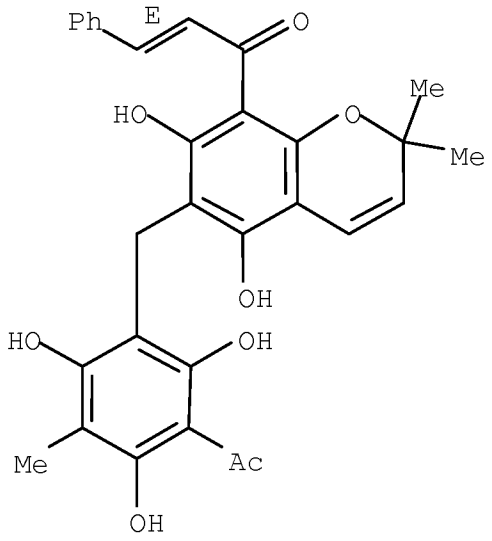

Figure 1.4: Structure of rottlerin

Rottlerin, a chemical compound abstracted from Mallotus philippinensis, was described as an inhibitor of PKC-δ and calmodulin kinase III (CaM-kinase III) (Gschwendt et al., 1994). Davies et al. (2000) observed the indirect effect of rottlerin on the activity of PKC-δ. McGovern and Shoichet (2003) claimed that rottlerin inhibited non-kinase enzymes. Rottlerin has been demonstrated to act as a mitochondrial uncoupler in rat parotid acinar cells (Soltoff, 2001) and in rat brain slices (Nguyen, Honours Thesis, 2004). Consequently, rottlerin had an inhibitory effect on the uptake of Rb^+ handled by the activity of Na^+/K^+-ATPase in rat cortical cultured astrocytes (Nguyen, Honours Thesis, 2004). However, the direct effect of rottlerin on the activity of Na^+/K^+-ATPase is unclear at this stage. The present study aims to investigate the effects of rottlerin on the activity of Na^+/K^+-ATPase from a preparation of cell-free homogenates.

1.5.3.4 Membrane lipids

It is widely recognized that the physical state of membrane lipids may influence the activity of many membrane bound enzymes (Kimelberg and Papahadjopoulos, 1972). The physical structure of the membrane lipids (Kimelberg, 1975) and their ordering (Sinensky et al., 1979) are reported to be an important determinant of Na^+/K^+-ATPase activity. Negatively charged phospholipids such as phosphatidylserine and phosphatidylinositol present in the preparation of purified Na^+/K^+-ATPase have been suggested to play a role in modulating enzyme activity (Kimelberg and Papahadjoupoulos, 1974; Roelofsen, 1981).

The activity of Na^+/K^+-ATPase of red blood cells is negatively related to the membrane cholesterol and phospholipids contents (Lijnen et al., 1992). Dietary supplementation with olive oil in normal subjects resulted in a decrease in the erythrocyte membrane contents of myristic, linoleic, palmitoleic and octadecatetraenoic acids, a fall in the cholesterol/phospholipids ratio, an increase in the oleic acid content and an increase in the erythrocyte Na^+/K^+-ATPase (Pagnan et al., 1989). Alterations in the proportion of unsaturated to saturated fatty acids in the acyl sidechains of membrane phospholipids influence the membrane fluidity and Na^+/K^+-ATPase activity (Kimelberg, 1975).

Corrocher et al. (1990) found an increase in the activity of the erythrocyte Na^+/K^+-ATPase in association with an increase in membrane arachidonic acid and unsaturated fatty acid. Lysophosphatidylcholines containing long-chain fatty acids such as myristoyl, palmitoyl, lauroyl, stearoyl and oleoyl acids inhibited the erythrocyte Na^+/K^+-ATPase activity (Lijnen et al., 1992).

1.5.4 Na^+/K^+-ATPase and glutamate

Activity of Na^+/K^+-ATPase has been seen to be altered in a number of brain diseases associated with an elevation of extracellular glutamate contents. Rapport et al. (1975) found 60% decrease in Na^+/K^+-ATPase in epileptic cortical patients. Brain regions with lower Na^+/K^+-ATPase activity appeared to be prone to seizure-like abnormalities (Haglund et al., 1985). Global loss of Na^+/K^+-ATPase was found in a transgenic mouse model of amyotrophic lateral sclerosis (Ellis et al., 2003). The ionic changes occurring as a result of ischemia and hypoglycemia (Hansen, 1985; Wieloch et al., 1984; Young et al., 1987) were consistent with a decrease in Na^+/K^+-ATPase activity. A pathological common in ischemic and traumatic insult was the extracellular accumulation of excitatory amino acid which led to excessive stimulation of glutamate receptors (Benveniste et al., 1984; Choi, 1988; Faden et al., 1989) and consequently, it contributed to the neuronal death caused by focal ischemia, hypoglycemia, epilepsy (Choi, 1990; Choi and Rothman, 1990; Rothman and Olney, 1986).

The elevation of extracellular glutamate concentrations can be a result of a reduction of glutamate uptake by glutamate transporters. Na^+/K^+-ATPase inhibitors ouabain and vanadate blocked the activity of glutamate-induced cultured astrocyte glutamate transporters (Abe and Saito, 2000). In brain slice studies, Na^+/K^+-ATPase blocker ouabain abolished glutamate uptake (Balcar and Johnston, 1972). There is a coupling between the activity of Na^+/K^+-ATPase and glutamate transporters. The extracellular glutamate is decreased over time in rat cortical astrocyte cultures (Abe and Saito, 2000) and the removal of the extracellular glutamate generates an increase in intracellular Na^+ concentrations, later maintained at a steady state by the activity of Na^+/K^+-ATPase

(Chatton et al., 2000). The activity of Na^+/K^+-ATPase has been reported to be proportional to glutamate stimulation (Pellerin and Magistretti, 1997).

1.5.5 The present study

1/. Examine the effects of Na^+/K^+-ATPase inhibitors, ouabain and digoxin, and a mitochondrial uncoupled inhibitor, FCCP (carbonyl Cyanide p-Trifluoromethoxyphenylhydrazone) on the distribution of GLAST at the cellular membrane from rat cortical cultured astrocytes.

2/. Investigate the effects of ouabain, digoxin and rottlerin on the activity of Na^+/K^+-ATPase from rat kidney homogenates and rat cortical cultured astrocyte homogenates.

3/. Test the effects of sodium deoxycholate (DOC), a detergent, on the activity of purified membrane Na^+/K^+-ATPase from rabbit kidney.

1.6 MONOLAYERS

Membrane lipids have been recognized to play an important role for protein functions. Alteration of membrane structure can influence the activity of the proteins. In the biological state, membranes are in disordered liquid crystalline phases. Understanding the structure and function of the membrane lipids is of interest in physics, chemistry and biology. Three typical models of biological membranes are planar lipid bilayers, vesicles (liposomes) and monolayers (Gennis, 1989). Lipid bilayers resemble a biomembrane more than monolayers (Singer and Nicolson, 1972). However, monolayers are a useful model system for the study of biological membranes (Tagami et al., 2006). Phospholipid monolayers resemble half of the lipid bilayer and have the advantages that the arrangement of the molecules can be controlled by changing the temperature and the molecular area or the surface pressure of the monolayers (Blume, 1979). The behaviour of the monolayer system is very similar to that of the respective bilayer system at a lateral

pressure of approximately 30 dyne/cm because at this pressure, the absolute area per lipid molecule and the area change in both systems are the same (Blume, 1979).

In the monolayer model, the spreading of amphiphilic phospholipids onto an aqueous phase (subphase) results in the formation of a two-dimensional monolayer on the water surface (Blume, 1979) because the phospholipids tend to absorb to the air/water interface. The phospholipids are hydrated by the interaction of water molecules with the polar head groups comprised of carbonyl and phosphate groups (Lairion and Disalvo, 2007). The hydration of the lipids has been suggested to contain 11-16 water molecules per phospholipid molecule associated with the membrane (Borle and Seelig, 1983). The monolayer of the phospholipids on the water surface reduces the surface tension of the subphase (Gutsmann et al., 2003). An air/hydrophobic layer and polar layer/aqueous subphase interfacial tensions make up the monolayer surface tension (Langmuir, 1933). The surface tension of pure water is 71.4 dyne/cm at 30^0C (Blume, 1979). The surface pressure is expressed as

$$\pi = \gamma_o - \gamma$$

γ_o is the surface tension of pure water and γ is the surface tension of the subphase covered with the monolayer (Blume, 1979). γ was assumed to be consisted of two terms, the surface tension, γ_h of the hydrocarbon/air interface and interfacial tension, γ_w of the head group/water interface (Scott, 1975; Scott and Cheng, 1977).

Natural and synthetic phospholipids have been found that they may exist in one of several different phases. Temperature has been used to trigger lipid phase transitions. The liquid crystal theory indicates that large deformations of the membrane can be accomplished with thermal energy at physiological temperatures (Helfrich and Jakobsson, 1990). Increasing temperature at the critical temperature, T_t, where the onset of rapid lateral diffusion of the lipid molecules from ordered to fluid transition occurred (Devaux and McConnell, 1972; Träuble and Sackmann, 1972) and was found to cause considerable expansion of the bilayer area (Phillips and Chapman, 1968). Higher order of the lipids,

on the other hand, is caused by a more extended hydrocarbon chains and decreased average lipid area per molecule (Huster et al., 1999). As well as, by temperature, lipid phase transitions can be induced by other factors such as pH and ionic strength of the aqueous subphase (Träuble and Eibl, 1974).

The membrane-bound enzyme Na^+/K^+-ATPase has been observed to be very sensitive to its lipid environment (Mayol et al., 1999; Murphy, 1990). The physical structure of the membrane lipids (Kimelberg, 1975) and their ordering (Sinensky et al., 1979) are reported to be an important determinant of Na^+/K^+-ATPase activity. Alterations in the proportion of unsaturated to saturated fatty acids in the acyl sidechains of membrane phospholipids influence the membrane fluidity and Na^+/K^+-ATPase activity (Kimelberg, 1975). Unsaturation of lipids decreases the lipid packing order in membranes and increases membrane fluidity (Stubbs et al., 1981; Keough et al., 1987; Cevc, 1991). An increase in membrane arachidonic acid and unsaturated fatty acid has been found to increase the activity of the erythrocyte Na^+/K^+-ATPase (Corrocher et al., 1990). Also, the incorporation of fatty acids into cell membranes influences membrane fluidity (Hashimoto et al., 1999) and enzyme activity (Gerbi et al., 1997; Mayol et al., 1999). Omegacoeur, a Mediterranean nutritional complement, consisting of ω3, ω6 and ω9 fatty acids, was found to increase Na^+/K^+-ATPase activity (Duran et al., 2001).

A chemical compound, rottlerin, and a detergent, DOC, have been recently found to stimulate the activity of Na^+/K^+-ATPase at low concentrations and inhibit the activity of the enzyme at higher concentrations (Cortas et al., 1989; in the present study). The aims of this study are to investigate the incorporation of these agents into the phospholipid monolayers of the synthetic DMPC lipids by using a Langmuir Trough at a constant area. Advantages of the constant-area method are speed and simplicity. The π-Γ (surface pressure-concentration) relationship can be measured directly from a constant delivery of the lipids and a collapse occurs sharply at the equilibrium pressure of hydrated lipids (MacDonald and Simon, 1987). The constant-area method is an unconventional procedure of π-A (surface pressure-area) isotherm which compresses the lipid monolayer after one addition of the lipids to the subphase. The difference of the constant-area

method from the π-A isotherm is continuing additions of a solution of phospholipids. The effect of the solvent used to dissolved the phospholipids in the constant-area method was observed to be lacking when both methods generated the same pressure (MacDonald and Simon, 1987). A solvent, chloroform, seems to have no effects on the monolayers because increasing aliquots of chloroform still produced a straight line at the plateau of saturating lipid concentrations (Lairion and Disalvo, 2007).

MATERIALS AND METHODS

2.1 MATERIALS

2.1.1 Sources of chemicals

Adenosine: Sigma Chemical Co. (St Louis, MO, USA)

Ammonia: from School of Chemistry, The University of Sydney

ATP: Sigma Chemical Co. (St Louis, MO, USA)

BSA: Sigma Chemical Co. (St Louis, MO, USA)

CCS: Hyclone (Logan, UT, USA)

Chloroform, 99.8%: Fluka (Buchs, SG, Switzerland)

Clozapine: Sigma Chemical Co. (St Louis, MO, USA)

D-aspartate: from Prof. Graham Johnston (Department of Pharmacology, The University of Sydney)

Digoxin: Sigma Chemical Co. (St Louis, MO, USA)

DMEM: Sigma-Aldrich (St Louis, MO, USA)

DMPC: Avanti Polar Lipids (Park ville, Australia)

DMSO: Sigma-Aldrich (St Louis, MO, USA)

DOC: Merck Pty. (Kilsyth, Vic, Australia)

EDTA: Sigma Chemical Co. (St Louis, MO, USA)

FCCP: Tocris Cookson Ltd (Bristol, UK)

Glucose: Sigma Chemical Co. (St Louis, MO, USA)

Glycerol: Sigma-Aldrich (St Louis, MO, USA)

Goat anti-mouse IgG-conjugated to AF 488: Molecular Probes (Eugene, OR, USA).

Goat anti-rabbit IgG-conjugated to AF 594: Molecular Probes (Eugene, OR, USA).

Haloperidol: Sigma Chemical Co. (St Louis, MO, USA)

HS: Trace Bioscientific (Castle Hill, NSW, Australia)

Imidazole: Sigma Chemical Co. (St Louis, MO, USA)

L-Histidine: Fluka (Buchs, SG, Switzerland)

Monoclonal mouse anti-GFAP: Sigma Chemical Co. (St Louis, MO, USA)

Na_3VO_4: Sigma Chemical Co. (St Louis, MO, USA)

Ouabain: Sigma Chemical Co. (St Louis, MO, USA)

P/S/G: Invitrogen (Carlsbad, CA, USA)

Paraformaldehyde: BDH chemicals (Kilsyth, Vic, Australia)

Polyclonal rabbit anti-GLAST: from Prof. David Pow (School of Biomedical Sciences, The University of Newcastle)

Poly-D-Lysine: Sigma Chemical Co. (St Louis, MO, USA)

Porcine trypsin: Sigma-Aldrich (St Louis, MO, USA)

Purified water (18.2 MΩ): Millipore Direct-Q system

RH421: synthesized at School of Chemistry, The University of Sydney

Rottlerin: Calbiochem (San Diego, CA, USA)

Saponin: Sigma-Aldrich (St Louis, MO, USA)

Sorbitol DMEM: Sigma Chemical Co. (St Louis, MO, USA)

Sorbitol: Sigma Chemical Co. (St Louis, MO, USA)

Sucrose: Sigma Chemical Co. (St Louis, MO, USA)

Trizma base: Sigma Chemical Co. (St Louis, MO, USA)

α,β-methylene ATP: Sigma Chemical Co. (St Louis, MO, USA)

2.1.2 Equipments

13 mm diameter coverslip: Menzel-Glaser, Germany

A 100 W arc mercury lamp: Osram, Germany

A 24-well plate: Sarstedt, Postfach, Nümbrecht, Germany

A 25 cm^2 cultured flask: Sarstedt, Postfach, Nümbrecht, Germany

A Langmuir-Blodgett Trough: Nima Technology Ltd., Coventry, England

A Pettier cooled CCD Axio Cam HRm camera: Zeiss, Jena, Germany

An AxioVision v 3.1 software (Carl Zeiss Vision GmbH): Zeiss, Jena, Germany

An IKA-VIBRAX-VXR shaker: Janke and Kunkel, Staufen, Germany

A RG 665 glass cut-off filter: Schott, Mainz, Germany

An UV-1601 UV-Visible spectrophotometer: Shimadzu, Tokyo, Japan

Hamilton Syringe: Hamilton, Baulkham Hills, NSW, Australia

ImageJ: Internet

R928 Photomultiplier: Hamamatsu, Japan

SF-61 Single Mixing Stopped-Flow System: Hi-Tech Scientific Ltd., Salisbury, UK
Spectra/Por dialysis tubing: Spectrum Laboratory, Rancho Dominguez, CA, USA
Square coverslips: Lomb Scientific, Taren Point, NSW, Australia
Zeiss Axioplan 2 microscope: Zeiss, Jena, Germany

2.1.3 Enzymes

Rabbit Na^+/K^+-ATPase-containing membrane fragments from Prof. Dr Hans-Jürgen Apell, Faculty of Biology, The University of Konstanz, Germany

2.1.4 Tissues

Rat kidney from Assoc. Prof. Paul Else, Department of Biomedical Science, The University of Wollongong, Australia

2.1.5 Animals

Sprague-Dawley male and female rats aged up to three postnatal days were purchased from Laboratory Animal Services, The University of Sydney.

This study was approved by the Animal Care and Ethics Committee, The University of Sydney.

2.2 METHODS

2.2.1 Cell cultures

2.2.1.1 Cerebral cortex dissection

Sprague-Dawley rat pups (1-3 day olds) were anaesthetised and sterilized in 70% ethanol. The rats were fixed on a sterilized dissection plate with pins. Dissecting tools were sterilized by 70% ethanol. The rat head skins and the skulls were removed to reveal the hemispheres in a fume hood. The cerebral cortices were removed and placed in Hanks balanced salt solution (containing 137 mM NaCl, 5.37 mM KCl, 4.17 mM $NaHCO_3$, 0.44 mM KH_2PO_4, 0.34 mM Na_2HPO_4, 5.55 mM glucose and pH 7.4). Meninges surrounding the cortices and other tissues such as olfactory bulbs, hippocampi, basal ganglia and underlying white matter were removed from the cortices under a light microscope. The clean cortices were sliced with a micro-scissor into 1-2 mm^2 pieces, then dissociated in 1 ml of Hanks balanced salt solution containing 0.25% trypsine and incubated at 37^0C for half hour in 5% CO_2.

After the incubation, the liquid was removed as much as possible from the cortical slices. Immediately, 6 ml of Dulbecco's Modified Eagle's Medium (DMEM) supplemented with 10% Cosmic Calf Serum (CCS) and 1% penicillin/streptomycin/glutamine (P/S/G) (DMEMs) were added to the slices to block the activity of trypsine. The suspension was centrifuged at 1200 rpm for 5 min. The pellet was re-suspended and centrifuged as previous. The pellet was homogenized in 1 ml of DMEMs by using a single pipette tip and a conjugated small-large pipette tips. The homogenized solution was transferred into a 25 cm^2 cultured flask pre-coated with 20 µg/ml of Poly-D-Lysine and added with DMEMs to make up 2.5 ml. The culture was incubated in a 5% CO_2 incubator at 37^0C. The medium of the cultured flask was replaced after 4 hour incubation and further replacements were done twice a week.

2.2.1.2 Purification of cultured astrocytes

The cultured cells are prepared from neonatal rats, at that time most of neurons are already postmitotic and lose the ability to divide whereas glial cells are still dividing (Hertz et al., 1998). Oligodendrocytes always grow on the top of the astrocyte layers (McCarthy and de Vellis, 1980). Therefore, the cultured astrocytes are necessary to be purified from the oligodendrocytes to obtain type 1 astrocytes equivalent of the normal cortical astrocytes in vivo whereas the existence and function of type 2 astrocytes related to oligodendrocytes are disputed in vivo (Hertz et al., 1998). The method of homogeneous cultured astrocytes is to apply constant shakes described by McCarthy and de Vellis (1980) to remove all oligodendrocytes. This purification was applied to the cultured cells when the cells reached confluence approximately at a 7^{th} date by shaking the cultured flasks on an IKA-VIBRAX-VXR shaker at 400 rpm for 4 hours at 37^0C. The purified astrocytes are predominantly grown in a medium with sorbital but not by contaminating cells (Wiesinger et al., 1991). After shaking, the medium of the cultures was exchanged by sorbital DMEM (DMEM without glucose supplemented with 10% horse serum (HS), 1% P/S/G and 25 mM sorbital) and the cultures were incubated in a 5% CO_2 incubator at 37^0C. The astrocyte cultures stay in this medium for 2-3 days. Then the cells were incubated with DMEMs and were ready for the experiment.

2.2.1.3 Transferation of the cells into coverslips

Before doing immunohistochemistry, the cultured astrocytes were transferred from the cultured flasks into 13 mm diameter coverslips sterilized by autoclave and dried in a fume hood. The attachment of the cells into the coverslips was induced by coating 20 µg/ml of Poly-D-Lysine on the coverslips before transferring the cells. The cultured cells were detached from the bottom of the cultured flasks by immersing the cells in 0.25% trypsin in HANK's solution for 3-5 min at 37^0C. The detachment of the cells from the flasks was stimulated by shaking. The suspension was immediately transferred into a 15 ml centrifuge tube and added 2 ml DMEMs. The centrifuge tube was centrifuged at 2000 rpm for 45 s. The pellet was re-suspended with 2 ml DMEMs and centrifuged at 2000

rpm for 2 min. The pellet was homogenized in 1 ml DMEMs by using a single pipette tip and a conjugated small-large pipette tips. The homogenate was filtered through a mesh and then transferred into the coverslips placed in a 24-well plate. The cells would attach the coverslips in 2-3 hours in a 5% CO_2 incubator at 37^0C. Then the medium of the cells was exchanged by the same fresh medium.

2.2.2 Immunohistochemistry

The cultured astrocytes in the 24-well plate were immersed in serum-free DMEM (sfDMEM) or brain buffer (containing 124 mM NaCl, 5 mM KCl, 1.2 mM KH_2PO_4, 1.2 mM $MgSO_4$, 1.2 mM $CaCl_2$, 26 mM $NaHCO_3$, 10 mM glucose and pH 7.4). The cells were incubated with drugs (glutamate transporter substrate, purinergic receptor agonists, dopamine receptor antagonists, ammonia/hyperammonia and Na^+/K^+-ATPase inhibitors). The control cells were incubated with the same medium (sfDMEM or brain buffer) without drugs. The incubation was lasted for 30 min in a 5% CO_2 incubator at 37^0C. The incubation was terminated by washing the cells with phosphate buffered saline (PBS) (containing 137 mM NaCl, 10 mM $Na_2HPO_4.12H_2O$, 1.76 mM KH_2PO_4 and pH 7.4). Each well of the 24-well plate was washed twice with 2 ml PBS for 5 min.

Then, the cells were fixed with 1% paraformaldehyde in PBS for 10 min at room temperature. The excessive paraformaldehyde was removed by washing twice with 2 ml PBS for 5 min. Next, the fixed cells were blocked with 1% bovine serum albumin (BSA) in PBS for 30 min. The blocking was terminated by washing the wells twice with 2 ml PBS for 5 min. After that, the coverslips were transferred into a new 24-well plate and incubated with 200 µl of each primary antibody for 2 hours at room temperature. The primary antibodies in this study were monoclonal mouse anti-GFAP, stained for morphology of astrocytes (1:400 dilution) and polyclonal rabbit anti-GLAST, stained for glutamate transporter GLAST (1:4000 dilution) in 0.05% saponin, 1% BSA in PBS. The incubation was terminated by washing the wells three times with 2 ml PBS for 10 min per wash.

After washing, the coverslips were transferred into a new 24-well plate and incubated with 200 µl of a secondary antibody (goat anti-mouse IgG-conjugated to Alexa Fluorescent 488) (AF 488) used to label GFAP (marking astrocytes) and 200 µl of another secondary antibody (goat anti-rabbit IgG-conjugated to Alexa Fluorescent 594) (AF 594) used to label GLAST protein glutamate transporters for 1 hr in the dark at room temperature. The secondary antibodies were diluted at 1:200 in 0.05% saponin, 1% BSA in PBS. The washing of the secondary antibodies was similar to that of the primary antibodies.

The labeled astrocytes were stored in a mounting medium (containing 20% glycerol in PBS). After washing the excessive antibodies, the coverslips were dried through a Kimwipe tissue and placed on slides. The cells were covered with the mounting medium and square coverslips and sealed by using nail polish around the edges of the square coverslips. The slides were kept at 4^0C and ready for viewing under a deconvolution microscope.

2.2.3 Deconvolution microscopy and image analysis

The labeled astrocytes were visualized on an automated Zeiss Axioplan 2 microscope, equipped with a fluorescence illumination lamp (100 W Hg lamp), a Pettier cooled CCD Axio Cam HRm camera and an AxioVision v 3.1 software (Carl Zeiss Vision GmbH). The images were undergone acquisition, deconvolution and analysis processes. In the acquisition process, the slide was covered with one drop of immersion oil to reduce the reflected light from the samples to the objective lens. The objective lenses were used at 40x magnification with 1.3 NA (numerical aperture), 0.17 mm WD (working distance) or 63x magnification with 1.4 NA, 0.09 mm WD. The emission wavelength from the dyes passed through the objective lens and was collected by appropriate filters fixed inside a filter cube. High quality narrow bandpass filters used for A488 and A594 excitation and detection are 41001 and 41004 filters, respectively. These filter sets include an exciter (HQ480/40), a beamsplitter (Q505lp) and emitter (HQ535/50) for A488 and an exciter (HQ560/55), a beamsplitter (Q595lp) and an emitter (HQ645/75) for A594. The samples

were scanned at distances of 0.325 μm (for 63x magnification) or 0.450 μm (for 40x magnification) in z direction. The image z-stacks were collected through the entire depth of the sample cells.

The image z-stacks were deconvolved to remove out-of-focus (background) signals by using a Regularized Inverse Algorithm method. The medial (in focus) sections (3-5 sections) from deconvolved z-stacks were used for image analysis. Each image represented a randomly selected single cell. The image was analyzed by using ImageJ software. The focused image was analyzed by drawing a line surrounding the cell and a line inside the cell apart from the boundary of the cell (the background) approximately 1.7 μm. The membrane was defined as the area between these two lines. The areas and mean fluorescence intensities of the cytoplasm and the whole cell were measured. The fluorescence values were subtracted from the fluorescence of the background. The ratio of fluorescence intensity (RFI) between the membrane and cytoplasm was calculated as an index of the distribution of GLAST between the membrane and cytoplasm. The RFI value of a single cell was defined as the mean of the RFI of the medial sections.

2.2.4 P_i (inorganic phosphate) assay of rat cultured astrocytes

Confluent rat astrocyte cultures around 1 month were washed with a cold homogenization medium (containing 250 mM sucrose, 5 mM EDTA, 20 mM imidazole, pH 7.4) and mechanically detached from the cultured flasks by a spatula. The cells were homogenized in the cold homogenization medium at 3% (w/v) by using a glass-glass homogenizer and stored in a freezer. Before doing the assay, the homogenates were thawed at room temperature for 15 min. Samples (150 μl) of the homogenates were preincubated for 10 min at 37^0C in the assay medium (containing 30 mM histidine, 4 mM $MgCl_2$, 128 mM NaCl and 20 mM KCl, pH 7. 4) either with or without 1 mM ouabain. KCl was omitted in the presence of ouabain. At the beginning of the preincubation, drugs (rottlerin or digoxin) were added to the suspension. Rottlerin dissolved in dimethyl sulfoxide (DMSO) was added to the solution at varying concentrations (5.0 μM → 200 μM in 1% DMSO final concentrations) while digoxin dissolved in ethanol was added to

the solution at 100 μM in 0.7% ethanol final concentrations. The controls were added with the same final concentrations of the solvents used to solubilize the drugs except without the drugs.

After 10 min preincubation, 3 mM ATP was added to the samples to initiate the activity of ATPase enzyme and the incubation was continued for 10 min. The activity was terminated by an addition of an equal volume of ice-cold 0.8 N perchloric acid. The samples were centrifuged at 1200g at 2^0C for 15 min. Aliquots of 250 μl from the centrifuged solutions were transferred into cuvettes and diluted with 250 μl of distilled water. The same volumes (500 μl) of the colour reagent were then added to the cuvettes. The colour reagent was prepared by dissolving 4g of $FeSO_4.7H_2O$ in 100 ml of a 1% ammonium molybdate ($(NH_4)_6Mo_7O_{24}.4H_2O$) solution and 3.3 ml of 98% H_2SO_4. This solution should be used within 2 hr after the preparation. The absorbance of the cuvettes was read after 10 min of the resulting colour at 750 nm by a UV-1601 UV-Visible spectrophotometer. The standard of inorganic phosphate assays was prepared from a stock solution of 1 mM of KH_2PO_4. Protein was assayed by the Lowry method (Lowry et al., 1951). Bovine serum albumin was used as a standard.

2.2.5 P_i (inorganic phosphate) assay of rat kidney

Rat kidney was homogenized in a cold homogenization medium at 2% (w/v) by using a glass-glass homogenizer and stored at -80^0C. Before doing the assay, the homogenates were thawed at room temperature for 15 min. Samples (50 μl) of the homogenates were then preincubated for 10 min at 37^0C in the assay medium either with or without 1 mM ouabain. KCl was omitted in the presence of ouabain. At initial time of the preincubation, drugs (rottlerin or digoxin) were added to the suspension. Rottlerin dissolved in DMSO was added to the solution at various concentrations (1.56 μM → 800 μM in 1% DMSO final concentrations) while digoxin dissolved in ethanol was added to the solution at varying concentrations (1.56 μM → 1.6 mM in 0.7% ethanol final concentrations). The controls were added with the same final concentrations of the

solvents used to solubilize the drugs except without drugs. The followings of the procedure were described in section (2.2.4).

2.2.6 Na^+/K^+-ATPase-induced RH421 fluorescent change from rabbit kidney

The kinetics of Na^+/K^+-ATPase was measured by rapidly mixing an enzyme-containing solution and an ATP solution. The enzyme-containing solution comprised a buffer (30 mM imidazole, 130 mM NaCl, 5 mM $MgCl_2$, 1 mM EDTA, pH 7.4), purified rabbit kidney Na^+/K^+-ATPase membrane fragments at 22 μg/ml, 300 nM RH421 and DOC at a variety of concentrations (0.1, 1.0, 2.0 and 5.0 mg/ml). The ATP solution was prepared by dissolving Na_2ATP in the same buffer at 1 mM concentration. These solutions were filled into 2 separate drive syringes of a stopped-flow apparatus. The temperature was maintained at 24^0 C. The solutions in the two drive syringes were mixed rapidly via a hydraulic ram driven by compressed air. The mixed solution in the observation chamber of the stopped-flow apparatus was excited by a 100 W arc mercury lamp at 577 nm and the fluorescence was measured at a right angle to the incident light beam at a wavelength ≥ 665 nm by using a RG 665 glass cut-off filter in front of a R928 multialkali photomultiplier. The kinetic data were collected and analysed using a software package from Hi-Tech Scientific Ltd.

2.2.7 Na^+/K^+-ATPase-induced RH421 fluorescent change from rat astrocytes

The kinetics of Na^+/K^+-ATPase was measured by rapidly mixing an enzyme-containing solution and an ATP solution. The enzyme-containing solution comprised a buffer (30 mM imidazole, 130 mM NaCl, 5 mM $MgCl_2$, 1 mM EDTA, pH 7.4), rat astrocyte cultured homogenates at 6.6 mg/ml, 300 nM (or 150 nM) RH421. Rat astrocyte cultured homogenates were prepared from confluent rat cultured astrocytes around 1 month. The cells were mechanically detached from the cultured flasks by a spatula and homogenized in a cold homogenization medium (containing 250 mM sucrose, 1 mM EDTA, 5 mM imidazole, 30 mM L-Histidine, pH 7.2) at 3% (w/v) by using a glass-glass homogenizer and stored in a freezer. The ATP solution was prepared by dissolving Na_2ATP in the

same buffer at 1 mM concentration. The followings of the procedure were described in section (2.2.6).

A drug, sodium orthovanadate (Na_3VO_4), was added to the enzyme–containing solution at 1.5 mM before the mixing while KCl was added to the ATP solution at different concentrations (0.62 mM, 4.88 mM, 14.1 mM) before the mixing. The stock solution of Na_3VO_4 was prepared at 7.5 mM by titrating an aqueous solution of the compound to pH 7.4 with HCl and then boiling the resultant yellow-colour solution until it became colourless, to remove polymerized vanadate species.

2.2.8 RH421 fluorescent transition in the presence of DMPC vesicles

A solution of DMPC (1,2-Dimyristoyl-sn-Glycero-3-Phosphocholine) vesicles and the dye RH421 (300 nM) was rapidly mixed with an equal volume of a buffer made the vesicles with or without the dye RH421 (300 nM). The mixture of the solutions and the observation of the fluorescent transition of the dye RH421 from the stopped-flow have been described in section (2.2.6). Single bilayer liposomes DMPC were prepared based on a modification of ethanol injection method of Batzri and Korn (1973). DMPC was dissolved in 100% absolute ethanol at 30 mM. The DMPC solution (1 ml) was slowly injected into a 10 ml warm buffer solution (containing 30 mM Trizma, 1 mM EDTA, 150 mM NaCl and adjust pH with HCl to 7.2) at 30^0C with a stirring bar over 10 min by using a Hamilton syringe. The diluting solution was transferred into dialysis tubing previously immersed in the buffer for a while. The sample was dialysed against the buffer solution at 30^0C for 2 days to remove the ethanol in the solution. The fresh buffer was exchanged twice. After 2 days, the DMPC vesicles were ready for the experiment.

2.2.9 Surface pressure-area (π-A) measurements

The surface pressure and area of an amphiphilic molecule were measured from the monolayer of amphiphilic molecules in a computerized Langmuir-Blodgett trough under constant area and constant temperature. The amphiphilic molecule used in this

experiment was DMPC, dissolved in chloroform at 1mg/ml. A solution of 10 µl of DMPC was spread on the surface of the subphase by using a Hamilton syringe each time after 10 min evaporation of the solvent. Before adding the new solution of DMPC, the surface pressure of the monolayer was measured by a paper Wilhelmy plate attached to a sensitive balance and the surface molecular area was measured from a program attached to the computerized Langmuir-Blodgett trough. The constant surface pressure of the monolayer was determined until no changes in the pressure after further adding the lipids. The area per molecular lipid at maximal pressure was estimated at the intersection of the equilibrium pressure and the steady slope of the surface pressure-molecules/$Å^2$ curve. The molecular area is the inverse of molecules per $Å^2$.

The subphase was pure (Millipore) water or an imidazole buffer (containing 30 mM imidazole, 130 mM NaCl, 5 mM $MgCl_2$, 1 mM EDTA and pH 7.4) with or without chemical compounds such as rottlerin or DOC. Rottlerin dissolved in 100% DMSO was diluted in the imidazole buffer subphase at different concentrations (0.1, 1.0 and 10.0 µM at 1% DMSO final concentrations). DOC was dissolved in pure water subphase. The temperature of the subphase was controlled by the heat generated from a water bath and measured by a thermometer.

2.2.10 Data analysis

The data obtained in Na^+/K^+-ATPase activity by measuring inorganic phosphate P_i production and the redistribution of glutamate transporter GLAST estimated by the ratio of fluorescence intensity (RFI) of GLAST between the membrane and the cytoplasm were analysed by using the Prism Software statistics package (Internet). Lines were fitted by non-linear/linear regression. Statistical comparisons were evaluated by using one way analysis of variance (ANOVA), Newman-Keuls test or unpaired t test. The data points collected from the stopped-flow experiments for the activity of Na^+/K^+-ATPase were fitted to an exponential time function by using the Origin Software.

RESULTS AND DISCUSSION